JOURNAL OF SYNCHROTRON RADIATION

ISSN 1600-5775

Received 1 October 2020
Accepted 21 December 2020

Edited by A. Momose, Tohoku University, Japan

Keywords: X-ray focusing; compound refractive lens; minimum X-ray beam size; nanofocusing; analytical theory.

Feasibility of X-ray beam nanofocusing with compound refractive lenses

V. G. Kohn[a,b] and M. S. Folomeshkin[b]*

[a]National Research Centre 'Kurchatov Institute', Moscow 123182, Russia, and [b]Shubnikov Institute of Crystallography of Federal Scientific Research Centre 'Crystallography and Photonics' of Russian Academy of Sciences, Moscow 119333, Russia. *Correspondence e-mail: folmaxim@gmail.com

A more general analytical theory of X-ray beam propagation through compound refractive lenses (CRLs) than the earlier study by Kohn [(2003). *JETP*, **97**, 204–215] is presented. The problem of nanofocusing with CRLs is examined in detail. For a CRL with a relatively large aperture the focusing efficiency is limited by the radiation absorption in the lens material. The aperture does not affect the focusing process and it is replaced by the effective aperture. The X-ray transverse beam size at the focus is then by a factor of $\gamma = \beta/\delta$ times smaller than the transverse beam size just behind the CRL. Here, δ and β are the real and imaginary parts of the CRL material refractive index $n = 1 - \delta + i\beta$. In this instance, to improve focusing efficiency, it is advantageous to decrease the CRL aperture and increase the photon energy E. However, with increasing photon energy, the material absorption decreases, which results in the CRL aperture impact on the transverse beam size. The latter leads to the fact that with a proper CRL length the beam size is independent of both the aperture and photon energy but depends only on the CRL material electron density and is approximately equal to $w_c = \lambda/(8\delta)^{1/2}$, where λ denotes the radiation wavelength, as predicted by Bergemann *et al.* [(2003). *Phys. Rev. Lett*, **91**, 204801].

1. Introduction

The complex refractive index for hard X-rays with photon energies from 5 to 100 keV may be written as $n = 1 - \delta + i\beta$ where $\delta = \delta_0 + \delta_1$. The first term δ_0 is defined by classical Thomson scattering and can be expressed as

$$\delta_0 = \frac{\lambda^2 r_0}{2\pi} N, \qquad r_0 = \frac{e^2}{mc^2}, \tag{1}$$

where $\lambda = hc/E$ is the wavelength of X-ray radiation, h is the Planck constant, c is the speed of light, E is the photon energy, e and m are the electron charge and mass, and N is the number of electrons per material unit volume.

The parameters δ_1 and β are defined by photoelectric absorption and Compton scattering, which are described by the quantum mechanical theory. There are other processes which give a very small contribution and can be neglected in our task. We note that $\delta_0 \gg \delta_1$. Therefore, for rough estimations it is sufficient to consider only δ_0. It is straightforward to verify that δ has a very small value compared with unity. For instance, for silicon and $\lambda = 0.1$ nm we have $\delta \simeq 3 \times 10^{-6}$ (Kohn, 2015). For this reason, X-ray focusing with refractive optics had been considered impossible for nearly 100 years after the discovery of X-ray radiation.

The situation changed by the mid-1990s when new radiation sources arrived; these included third-generation synchrotron light sources (*e.g.* ESRF, APS, SPring-8) and free-electron

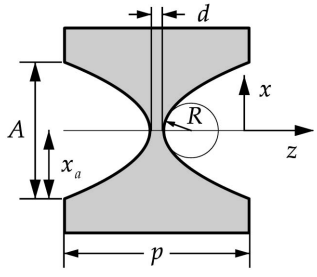

lasers. Fourth-generation synchrotron facilities are also emerging nowadays. Such sources may produce X-ray beams with very small lateral sizes, and thus even refractive lenses with relatively small effective apertures may be beneficial.

Additionally, compound refractive lenses (CRLs) have become widespread. CRLs are composed of elements with a parabolic profile of the radius of curvature R at the apex, which should be as large as possible to simplify their fabrication process. Refraction is enhanced by using the large number of elements placed close together in a row along the beam path. This concept was initially implemented by Snigirev *et al.* (1996) for the one-dimensional lens fabricated as the set of cylindrical holes in aluminium and has become widespread later. Two-dimensional lenses with parabolic shape appeared in the work by Lengeler *et al.* (1999).

A method of microstructuring (microfabrication) technology on a silicon surface, which is widely applied in the computer industry, has been developed since 2001 for manufacturing one-dimensional planar lenses (Grigoriev *et al.*, 2001; Schroer *et al.*, 2003). Microstructuring technology makes it possible to produce CRLs with relatively small curvature radius and aperture, and thus with small size along the beam path. It is these lenses that are currently capable of focusing X-rays to nanometre dimensions. Fig. 1 presents the main parameters of the CRL individual elements in the coordinate plane (x, z), where z stands for the optical axis. Here, A is the aperture, R is the curvature radius of the parabolic profile at the apex, and d is the thickness of the thin layer of material between two parabolic surfaces (minimal thickness).

The length of the individual lens elements along the z-axis is defined as $p = d + A^2/4R$. In the general case, the CRL can be composed of up to several hundred individual elements. In this paper, three examples of CRLs are considered with the following parameters in micrometres: $A = 50$, $R = 6.25$, $p = 102$ for the first example; $A = 30$, $R = 3.75$, $p = 62$ for the second; $A = 10$, $R = 1.25$, $p = 22$ for the third. The minimal element thickness $d = 2$ is equal for all three examples of CRLs.

The first CRLs example have been used, inter alia, in the studies on the bi-lens (Snigirev *et al.*, 2009) and six-lens (Snigirev *et al.*, 2014) interferometers. The second CRLs have been used to build up a 30-lens interferometer (Lyubomirskiy *et al.*, 2016). There are no published experimental results for the third CRLs, but the lenses have been fabricated and exist.

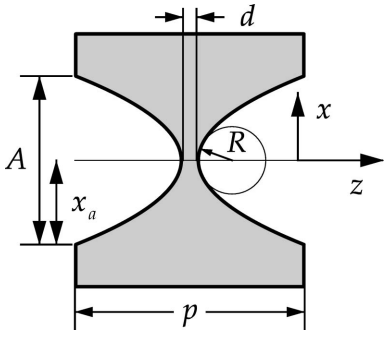

Figure 1
Parameters of one element of an X-ray compound refractive lens.

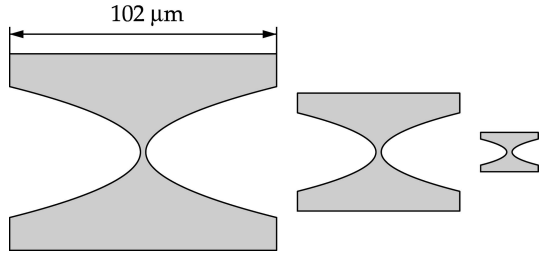

Figure 2
Individual CRL elements with accurate relative sizes of the three examples of CRLs covered in the paper.

Fig. 2 shows these three examples with their accurate relative sizes.

The question of the limit to the beam focusing effect using CRLs requires the development of an adequate theory capable of making rapid assessments with controlled accuracy. The present paper analyses different theory approximations and the degree of their accuracy. The major outcome of the work is the prediction of the minimal spot size of the focused beam.

We note that in the paper by Schroer & Lengeler (2005) the adiabatically focusing CRL was proposed and theoretically evaluated. However, such CRLs have not been manufactured so far. We think that adiabatical CRLs will not be used in the future for many reasons. That is why we do not analyze these CRLs in this paper. Instead, we will consider cascade CRLs in the following publications.

The next section considers various approximations of the theory and analyses their accuracy by means of calculating ray trajectories using geometrical optic laws (ray-tracing approach). High precision of the examined approximations is demonstrated. In the third section, the analytical theory of a continuously refractive lens without considering its aperture is presented. The fourth section describes an iterative calculation method and the theory refinement for the case when the CRL aperture influences the result of beam focusing.

2. Ray trajectories and main approximations of the theory

As shown in Fig. 1, planar lenses focus radiation in the plane (x, z), and, since X-ray refraction is weak, the paraxial approximation can be used with high accuracy. In this case, the surface of the constant wave phase φ is very close to the direction normal to the beam traveling direction, which we consider as the z-axis. The angle θ between the radiation ray and the axis z can be described using the simple formula

$$\theta = K^{-1}\frac{\mathrm{d}\varphi}{\mathrm{d}x}, \qquad K = \frac{2\pi}{\lambda}, \tag{2}$$

where x denotes the coordinate along the direction normal to the z-axis. It is then straightforward to calculate the angle change at the air–material and material–air interfaces. For a lens with constant material density, the x-dependence of the phase shift inside the lens is equal to $\Delta\varphi = -K\delta\Delta z$, where Δz is the ray path inside the lens material.

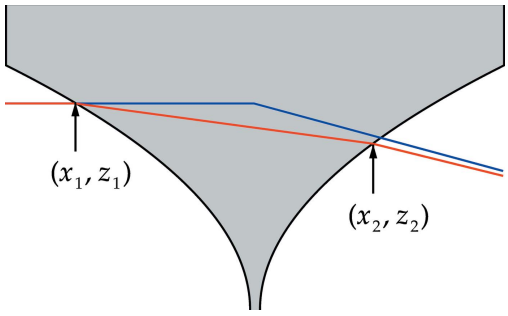

Figure 3
Trajectories of X-rays for the accurate solution of the problem (red line) and in the approximation of compressed lenses (blue line).

For the first air–material interface, we consider Δz as the distance from this interface to the lens center along the z-axis as $\Delta z = x^2/2R$. We have the same dependence for the second material–air interface. Therefore, the angle change on each interface is the same and can be expressed as

$$\Delta\theta = -\delta\,\frac{x}{R}. \tag{3}$$

Figure 3 illustrates the discussed situation for the individual lens element by the red line. The specific calculation of the ray trajectory in the lens element can be carried out using the formulas presented below.

Consider a beam with the parameters $z_0 = -p/2$, x_0, θ_0 at the lens entrance. The coordinates of the point where the ray enters the lens material are $z_1 = z_0 + z_r$, $x_1 = x_0 + z_r\theta_0$, where

$$z_r = \left[\left(B^2 - 4AC\right)^{1/2} - B\right]/2A. \tag{4}$$

Here,

$$A = \theta_0^2/2R, \quad B = 1 + x_0\theta_0/R, \quad C = z_0 + d/2 + x_0^2/2R. \tag{5}$$

Note that $A > 0$, $B > 0$ but $C < 0$. At this point the angle defining the ray direction changes to have the value $\theta_1 = \theta_0 - x_1\delta/R$.

The coordinates of the second point, where the beam exits the material, are $z_2 = z_1 + z_r$, $x_2 = x_1 + z_r\theta_1$, where

$$z_r = \left[B - \left(B^2 - 4AC\right)^{1/2}\right]/2A. \tag{6}$$

Here,

$$A = \theta_1^2/2R, \quad B = 1 - x_1\theta_1/R, \quad C = d/2 + x_1^2/2R - z_1. \tag{7}$$

Note that now $A > 0$, $B > 0$, $C > 0$ and the ray direction angle changes to $\theta_2 = \theta_1 - x_2\delta/R$. At the lens end (just behind the one CRL element) we have $z_3 = p/2$, $x_3 = x_2 + (z_3 - z_2)\theta_2$, $\theta_3 = \theta_2$.

Equations (4)–(7) allow the accurate calculation of ray trajectories in the individual CRL element. Fig. 3 (red line) shows the case of the first example of the considered CRLs (p = 102 µm), $\theta_0 = 0$ and $\delta = 0.02$. The δ value is very large compared with the actual values of order 10^{-6}. For a better view the vertical size in the figure was twice increased. If there are other elements along the optical axis, the calculation can be repeated with the new boundary conditions equal to the beam parameters at the end of the previous element. Such calculation can be easily carried out for the ray trajectories in all the CRL elements. This approach is similar to the ray-tracing calculations which were used for the CRL by Protopopov & Valiev (1998) and then by many authors. For example, one can look for the well known program *SHADOW* (Sanchez del Rio *et al.*, 2011). Nevertheless, the general solution of the Maxwell equations for the CRL with the parabolic profile appears to be rather complicated.

However, it is not necessary to look for the exact solution to the problem, since simpler approximations can be used due to a very small value of δ. In this paper, we consider two approximations, which are the opposite extreme cases. These approximations are used in more accurate wave-propagating calculations.

We can call the first case the phase-contrast imaging approximation where the thickness of the object is small and neglected. One takes into account the complex phase shift only. This approximation can also be called the compressed lens approximation, because we assume that the thickness of the single element is zero, and the element is described as the straight line perpendicular to the z-axis with $z = 0$. Nevertheless, the X-ray wave phase shift upon crossing this line is the same as for the real individual element, *i.e.* $\Delta\varphi = -K\delta x^2/R$. Such an approach was used in the theory of photonic crystal imaging (Kohn *et al.*, 2014; Kohn, 2018). It is similar to the multi-slice method used in the theory of transmission electron microscopy.

Thus, in this approximation for the individual element, the radiation ray changes direction only at a single point with the coordinates $x_1 = x_0 + \theta_0 p/2$, $z_1 = 0$. The angle between the ray and the optical axis changes to $\theta_1 = \theta_0 - 2x_1\delta/R$, and at the end of the element we have $x_2 = x_1 + \theta_1 p/2$, $z_2 = p/2$, $\theta_2 = \theta_1$. The final result can be expressed as

$$x_2 = x_0\left(1 - \frac{\delta p}{R}\right) + \theta_0 p. \tag{8}$$

The ray trajectory in the single lens element for this case is presented in Fig. 3 by the blue line. Both the red and the blue lines are given for the same parameters. One can see that, if the parameter δ has a very large value compared with the real situation, the blue trajectory may vary from the red one. However, the difference becomes very small for the actual values of δ.

We define the second case as the continuous refraction approximation or the distributed lens approximation. Now we consider the lens as the medium of the constant density along the z axis. However, in this case, the material density depends on the x coordinate in such a way that the phase shift is also equal to the correct value $\Delta\varphi = -K\delta x^2/R$. It is easy to verify that in this approximation we have $\varphi = \varphi_0 - K\delta(x^2/pR)(z - z_0)$ for any point in the lens material. It should be noted that the real lens has a constant density, and only the material thickness varies along the x-axis, while in the continuous refraction approximation the density changes, but the lens thickness is constant.

This case was considered by Kohn (2002, 2003), where an analytical solution for the wave equation was obtained. In the second approximation, the ray trajectory is a smooth curve for which we can write

$$\frac{dx}{dz} = \theta(z), \quad \frac{d\theta}{dz} = -\frac{x}{L_c^2}, \quad L_c = \left(\frac{pR}{2\delta}\right)^{1/2}. \tag{9}$$

The parameter L_c was introduced in the theory presented by Kohn (2002, 2003) where its physical meaning was discussed. The solution to $x(z)$ can be expressed in analytical form

$$x(z) = x_0 \cos(z/L_c) + \theta_0 L_c \sin(z/L_c). \tag{10}$$

Here, the z-coordinate starts at the entrance of the elementary lens. The expression for angle $\theta(z)$ can be found by differentiating (10) over z. Interestingly, equation (10) gives the same value as in the case of the phase contrast approximation for the x coordinate at the end of the lens ($z = p$), provided that $p \ll L_c$. However, it should be noted that the condition $p \ll L_c$ is met only for the small values of δ.

For a stack of elementary lenses forming a CRL, the exact calculation of ray trajectories, as well as the calculation in the phase-contrast approximation, is an iterative procedure. As for the continuous refraction approximation, equation (10) immediately gives the result for any number of elements when $z = N_1 p$, where N_1 stands for the number of elements in the CRL. We will consider N_1 as a free parameter.

To demonstrate the accuracy of both approximations, we consider the case where the CRL focuses the beam at its end. In this case we obtain the maximum change of the trajectories inside the CRL. We calculate three curves of the ray trajectories: one for the exact trajectory, which takes into consideration refraction at each boundary, and two curves for the approximations considered above. We choose $x_0 = x_a = A/2$, $\theta_0 = 0$ as the initial coordinates and choose the number of lenses N_1 that gives the minimal x coordinate greater than zero. Calculations were made for different photon energies and for all three examples of CRLs.

It is sufficient to compare the coordinates X_n at the end of the trajectories, where $n = 0$ is applied for the case of the exact calculation, and $n = 1, 2$ corresponds to the first and second approximations. The main parameters are the relative difference in the coordinates $\varepsilon_1 = (X_1 - X_0)/x_0$ and $\varepsilon_2 = (X_2 - X_0)/x_0$. We consider three values of photon energy: $E = 10$, 30 and 50 keV. We have obtained that the numbers of CRL elements N_1 are approximately the same for all three examples of CRLs because they have similar form (see Fig. 2). The specific values are: $N_1 = 118$, 360 and 602; $\varepsilon_1 \times 10^7 = -38$, -4.3 and -1.5; $\varepsilon_2 \times 10^7 = 68$, 7.4 and 2.7, for the corresponding photon energy values pointed out above.

From the above results, we can conclude that in the first approximation the trajectory changes more rapidly, while in the second one it changes less rapidly compared with the accurate trajectory. The accurate trajectory lies between the considered approximations. The difference decreases with increasing photon energy and it is highest for the lowest considered energy $E = 10$ keV. This is because the parameter δ is inversely proportional to the square of photon energy [see equation (1)]. Nevertheless, the main parameter of accuracy does not exceed the value 5×10^{-6} even for $E = 10$ keV.

The calculation results reveal that both approximations have a sufficiently high degree of accuracy especially for the high photon energies. It should be mentioned that low-energy X-ray beam focusing is less efficient due to strong radiation absorption. It is interesting to note that all three types of analyzed lenses focus the beam at their end with approximately the same number of individual elements N_1. Slight variations occur since the minimal element thickness d does not change with the decreasing element length p. These minor changes are, however, not significant.

Thus, we can assume that the considered approximations are fully applicable for the analysis of the CRLs, presented in the first chapter. The first approximation for the individual CRL element is consistent with the commonly known phase-contrast imaging theory (Snigirev *et al.*, 1995; Argunova & Kohn, 2019). It neglects the ray path change inside the object and takes into account only the trajectory angle change through the total phase shift and absorption. In this instance, the phase object can be described by means of the transmission function, independent of the illuminating wavefield.

The second approximation was first considered by Kohn (2002, 2003) in order to obtain the analytic solution of the Maxwell equations for a more complex CRL propagator. This solution was used to derive the simple analytic expressions that allow estimating the focused beam parameters, which is useful for an experimental scheme to be easily determined. The next section discusses this approximation in more detail.

3. Analytical theory of focusing X-rays by the continuously refractive lens

The analytic solution of the Maxwell equations for the model of the continuously refractive lens in the two-dimensional case has been widely discussed in the earlier work (Kohn, 2003). The following is a brief overview of this theory basic equations for the one-dimensional focusing of the beam in the (x, z)-plane. The general solution of the Maxwell equation for the monochromatic X-ray wave electric field $E(x, z)$ can be expressed as $E(x, z) = \exp(iKz)\, B(x, z)$. Here, the function $B(x, z)$ describes the relatively slow transfer of the wavefield transverse dependence along the z-axis, while the phase factor oscillates rapidly.

In the paraxial approximation and for the specified CRL model, function $B(x, z)$ satisfies the following equation,

$$\frac{dB}{dz} = -iK_0 B - iK\frac{x^2}{2z_c^2} B + \frac{i}{2K}\frac{d^2 B}{dx^2}, \tag{11}$$

where the z-coordinate origin is located at the CRL entrance, and

$$K_0 = K\eta\frac{d}{p}, \quad z_c = \left(\frac{pR}{2\eta}\right)^{1/2}. \tag{12}$$

Here, $\eta = \delta - i\beta$, the parameter β determines the absorption of the radiation in the lens material. Note that in the given form,

equation (11) is valid only within the CRL aperture, while outside of it (*i.e.* for $x > x_a = A/2$) x is to be replaced with x_a.

We focus only on the case of long and highly absorbing CRLs. Therefore, the function B becomes zero at the aperture boundary, and the aperture itself has no impact on the result. The CRL length equals $L = N_1 p$. The general solution of equation (11) can be written as a convolution,

$$B(x, L) = C_0 \int \mathrm{d}x_1 \; P_L(x, x_1)\, B(x_1, 0), \tag{13}$$

where $C_0 = \exp(-iK_0 L)$. The CRL propagator $P_z(x, x_1)$ satisfies equation (11) without the first (constant) term at the right-hand part, and the boundary condition $P_0(x, x_1) = \delta(x - x_1)$, where $\delta(x)$ stands for the Dirac delta function. In the work by Kohn (2003) this function has been shown to have an analytic form,

$$P_L(x, x_1) = \frac{1}{(i\lambda z_c\, s_L)^{1/2}} \exp\left[i\pi \frac{\left(x^2 + x_1^2\right) c_L - 2x x_1}{\lambda z_c\, s_L}\right] \tag{14}$$

where

$$c_L = \cos(L/z_c), \quad s_L = \sin(L/z_c). \tag{15}$$

If the wavefunction $B(x, 0)$ at the CRL entrance is known, we can obtain the new wavefunction $B(x, L)$ at the end of the CRL from equation (13).

Now consider a more general problem when the CRL is illuminated by a point source with the coordinate x_o at the distance r_o from the lens entrance. Of interest is the wave amplitude at the point with the coordinate x_i located at the distance r_i from the CRL end. Such a function $G(x_i, x_o)$ can be called the CRL image propagator. It is convenient to calculate the dimensionless intensity as the ratio of the radiation intensity at the observation point to the intensity of the X-ray radiation in front of the CRL.

In this case, the image propagator can be expressed as

$$G(x_i, x_o) = C_n C_0 \int \mathrm{d}x\, \mathrm{d}x_1 \; P(x_i - x, r_i) \times P_L(x, x_1)\, P(x_1 - x_o, r_o), \tag{16}$$

where $C_n = (i\lambda r_o)^{1/2}$, and the Fresnel propagator

$$P(x, r) = \frac{1}{(i\lambda r)^{1/2}} \exp\left(i\pi \frac{x^2}{\lambda r}\right) \tag{17}$$

describes propagation of the radiation in empty space.

Note that the factor C_0 does not affect the intensity distribution and has only a supplementary meaning. It merely reduces the radiation intensity after the lens due to the radiation absorption in the thin parts of the elementary lenses. For the sake of simplicity, we will omit this factor and consider it as equal to unity. For the more accurate calculations, the absorption can be easily incorporated by the factor $M_a = \exp(-\mu d N_1)$, where $\mu = 2K\beta$ is the X-ray absorption coefficient of the lens material.

It was demonstrated by Kohn (2003) that the function (16) also has an analytical solution, which we present here in an alternative form, namely

$$G(x_i, x_o) = \left(\frac{r_o}{r_g}\right)^{1/2} \exp\left(i\pi \frac{x_i^2 C_o + x_o^2 C_i - 2x_i x_o}{\lambda r_g}\right) \tag{18}$$

where

$$C_{i,o} = c_L - \frac{s_L}{z_c} r_{i,o}, \quad r_g = (r_i + r_o)\, c_L + \left(z_c - \frac{r_i\, r_o}{z_c}\right) s_L. \tag{19}$$

The dimensionless relative radiation intensity is $I(x_i, x_o) = |G(x_i, x_o)|^2$. It is obvious that for $r_i = 0$, $r_o = 0$ we can find $G(x_i, x_o) = P_L(x_i, x_o, L)$ from equation (18). It can also be shown that the following evident physical relations are satisfied,

$$\int \mathrm{d}x_o \; G(x_i, x_o, r_i, r_o)\, P(x_o - x_s, r_s) = G(x_i, x_s, r_i, r_o + r_s), \tag{20}$$

$$\int \mathrm{d}x_i \; P(x_d - x_i, r_d)\, G(x_i, x_o, r_i, r_o) = G(x_d, x_o, r_d + r_i, r_o). \tag{21}$$

Equation (18) has limited scope and is valid only if the result does not depend on the CRL aperture, *i.e.* the full width at half-maximum (FWHM) of the Gaussian beam at the end of the CRL is less than half the CRL aperture. If the condition is not met, the integration cannot be done for infinite limits. It is demonstrated below that the cases when this condition is not satisfied do exist. Therefore, the estimation of the CRL effective aperture size is of great importance.

On modern synchrotron radiation sources and free-electron lasers, the distance r_o is typically large; thus, let us consider the extreme case $r_o \to \infty$, which corresponds to the incident plane wave. In this regard, the result does not depend on the coordinate x_o and is equal to

$$I(x_i) = \left|\frac{z_c}{z_i}\right| \exp\left(\mathrm{Im}\left[\frac{s_L}{z_i}\right] K x_i^2\right), \quad z_i = z_c\, c_L - r_i\, s_L. \tag{22}$$

The effective aperture A_e of the lens (Kohn, 2017) is defined as the integral of (22) for any value of r_i. Below, we take into account the fact that $\gamma = \beta/\delta \ll 1$ and restrict ourselves to the linear in γ approximation. Consequently, $z_c \simeq L_c(1 + i\gamma/2)$,

$$s_L \simeq S_L - i\gamma u C_L/2, \quad c_L \simeq C_L + i\gamma u S_L/2, \tag{23}$$

where

$$u = L/L_c, \quad C_L = \cos u, \quad S_L = \sin u. \tag{24}$$

Integrating with $r_i = 0$ we have

$$A_\mathrm{e} = \left(\frac{\lambda F_L}{2\gamma\alpha_L}\right)^{1/2}, \quad F_L = \frac{L_c}{S_L}, \quad \alpha_L = \frac{1}{2}\left(C_L + \frac{u}{S_L}\right). \tag{25}$$

This value is valid for any distance r_i.

The focusing condition occurs if $r_i = r_f$ where r_f is the distance for which the quantity $I(0)$ in equation (22) has the maximum value. It is easy to verify that the maximum is achieved when the real part of the parameter z_i equals zero. Linear in γ approximation leads to the next equation for the

focus distance $r_f = F_L C_L$. At this distance equation (22) will be as follows,

$$I(x_i) = \frac{1}{\gamma\alpha_L}\exp\left(-\frac{Kx_i^2}{\gamma F_L \alpha_L}\right). \quad (26)$$

We define the beam transverse size at the focus w_f as the FWHM of this Gaussian function and obtain

$$w_f = C_w(\gamma\lambda F_L\alpha_L)^{1/2}, \quad C_w = (2\ln 2/\pi)^{1/2} = 0.664. \quad (27)$$

In the limit of the thin CRL ($u \ll 1$) we apply the approximations $C_L = 1$, $S_L = u$. Then r_f becomes equal to $f = L_c^2/L = R/(2N_l\delta)$ and we obtain from (25) and (27) a well known result (Kohn, 2003, 2009, 2012, 2017), namely, $w_f = C_w(\gamma\lambda f)^{1/2}$, $A_e = C_a C_w(\lambda f/\gamma)^{1/2}$, where $C_a = 1/(2^{1/2}C_w) = 1.064$.

The integral in infinite limits A from the Gaussian function with maximum value I_m and FWHM w is known to be equal: $A = C_a I_m w$. Let us apply this equation to the case of the focus distance. We obtain that the maximum value of the intensity is $I_m = \gamma^{-1}$. On the other hand, the maximum value of the intensity at the end of the CRL is $I_m = 1$. Let w_0 be the FWHM at the end of the CRL. Then we obtain that $w_f = \gamma w_0$. This means that if the beam size is defined by the absorption, the CRL compresses the beam to become of γ times smaller size. Consequently, the parameter γ can be called the CRL focusing efficiency.

Of particular interest is the minimum beam size attainable with the use of CRLs. From a physical point of view, it is clear that the minimal size corresponds to such a CRL length for which the beam is focused at the end of the CRL, *i.e.* when $r_i = 0$. This condition is met for $L = (\pi/2)L_c$, and in this case from the general equations we have

$$w_f = 0.589(\gamma\lambda L_c)^{1/2}, \quad I_f = 1.273/\gamma. \quad (28)$$

Here, I_f denotes the maximum value of the relative radiation intensity at the focus. The effective aperture is determined from the above equations in a standard way,

$$A_e = C_a w_f I_f = 0.798(\lambda L_c/\gamma)^{1/2}. \quad (29)$$

Note that $0.589 = (\ln 2/2)^{1/2}$, $0.798 = (2/\pi)^{1/2}$, $1.273 = 4/\pi$.

The resulting equations lead to a few interesting conclusions. First, the beam size at the focus is by a factor of 0.74γ smaller than the effective aperture, even for the extremely long CRL. Therefore, the beam is compressed more efficiently for hard X-rays having a shorter wavelength λ because γ is an increasing function of λ. It is also clear that the CRL length should be minimal, which can be achieved by reducing the CRL aperture.

For real CRLs, $L = N_l p$ and it is necessary to choose the maximum number of elementary lenses $N_l = N_m$, which gives the closest value of L less than $(\pi/2)L_c$. However, in practice, the increase in number of elements N_l more than $N_m/2$ does not significantly reduce the beam size. This is due to the fact that the beam is weakly refracted in the vicinity of the optical (CRL) axis, and the beam converges to the focus even in empty space. This conclusion follows from the results of our computer simulations.

Table 1
Calculated values of the beam size at the focus and other parameters for the CRLs with length $L = L_o$.

CRL N	1	2	3
E = 10 keV, γ = 0.015			
L_c (mm)	8.05	4.86	1.67
N_l	61	61	59
A_e (μm)	7.23	5.61	3.29
$2A_e/A$	0.3	0.4	0.7
w_f (nm)	93	72	42
E = 30 keV, γ = 0.0018			
L_c (mm)	24.4	14.7	5.06
N_l	187	186	180
A_e (μm)	20.7	16.1	9.42
$2A_e/A$	0.8	1.1	1.9
w_f (nm)	32	25	15
E = 50 keV, γ = 0.00091			
L_c (mm)	40.6	24.6	8.44
N_l	313	310	301
A_e (μm)	29.4	22.9	13.4
$2A_e/A$	1.2	1.5	2.7
w_f (nm)	23	18	10

Let us consider the CRL length which is twice as small compared with the above case and equals $L_o = (\pi/4)L_c$. Direct calculation shows that the focal length $r_f = L_c$. Further, we have

$$w_f = 0.753(\gamma\lambda L_c)^{1/2}, \quad I_f = 1.1/\gamma, \quad A_e = 0.881(\lambda L_c/\gamma)^{1/2}. \quad (30)$$

In comparison with the previous result, the beam size has increased by a factor of 1.3, the relative intensity has slightly decreased, and the effective aperture has slightly increased. The distance from the CRL entrance to the focusing point is now equal to $1.78L_c$ compared with the value $1.57L_c$ for the CRL focusing the beam at the end. Thus, we have a slight difference in beam parameters with the twice decreased number of CRL elements, which is significant from a practical standpoint (such a CRL has half the cost).

Table 1 lists the results of the accurate calculations made using general expressions (26)–(28) for the three examples of CRLs with the specific value of N_l closest to but less than $N_m/2$. The second line from the bottom for each energy represents the applicability of the calculations. The CRL aperture does not influence the result if $A_e < 0.5A$. This condition is met for all three examples of CRLs at low photon energies and is not fulfilled at high energies, particularly for the CRLs with the small aperture. When the condition is not fulfilled, estimations for the focus beam size produce invalid values. First, in this case, the intensity distribution at the focus is not described by the Gaussian function, and additional peaks may appear. As regards the FWHM of the central peak, it typically exceeds the predictions of expressions (26)–(28) when the above criterion is not met.

We can rewrite expression (30) for the lateral beam profile in an alternative form using the expression of L_c via the aperture A, namely, $L_c = Ah/(8\delta)^{1/2}$, where $h = [p/(p-d)]^{1/2} \simeq 1 + 2dR/A^2$ is the parameter which takes into account the

minimal thickness of the CRL element. It is slightly less than unity. The new expression is as follows,

$$w_f = 0.753(\gamma A h\, w_c)^{1/2}, \quad w_c = \lambda/(8\delta)^{1/2}. \tag{31}$$

The parameter w_c was introduced as the critical size of the focused beam by Bergemann *et al.* (2003), who claimed that it is impossible to focus the X-ray beam to a size less than w_c using any focusing device. However, it is seen from expression (31) that such focusing should be possible if we have $\gamma A < w_c$. The problem is that in this case expression (31) becomes not applicable because $A_e > A/2$.

4. Iterative calculation in the phase-contrast imaging approximation and refinement of the analytical theory

A more complicated calculation of X-ray nanofocusing can be performed using the iterative method in the first approximation outlined above, similar to the phase-contrast imaging approach. In this case, the following calculation scheme is used. The illuminating radiation is defined by the function $B_0(x) = (i\lambda r_o)^{1/2} P(x, r_o + p/2)$, which we multiply by the transmission function of the first CRL element, expressed as

$$T(x) = \exp\left(-i\pi \frac{x^2}{\lambda f}[1 - i\gamma]\right), \quad f = \frac{R}{2\delta}, \tag{32}$$

if $|x| < x_a = A/2$. For the values of x for which the condition $|x| > x_a$ is satisfied, we have $T(x) = T(x_a)$. The latter value has no impact on focusing and is substantial only for large distances from the focus. Note that in equation (32) we ignore the absorption in the thin parts of the CRL once again, similarly to the continuously refractive lens approximation.

Now we calculate the radiation wavefunction in front of the second lens element using the following expression,

$$B_{n+1}(x) = \int \mathrm{d}x_1\; P(x - x_1, p)\, T(x)\, B_n(x), \tag{33}$$

for $n = 0$, and then we repeat the calculation for $n = 1, \ldots, N_l - 2$, where N_l is the number of CRL elements. For $n = N_l - 1$, the calculation using (33) is repeated once again with the argument p substituted by $r_i + p/2$. The convolution integral in equation (33) is calculated by applying the Fourier transform using the fast Fourier transform algorithm (Cooley & Tukey, 1965) with the data size $N = 2^m$, where m is an integer.

Figure 4 shows the intensity distributions of the radiation immediately after the third CRL example for $E = 50$ keV (last column of Table 1 for this energy). The calculations were performed for $r_o = 50$ m using the iterative method discussed in this section (black line) and under the continuous refraction approximation using general expression (18) (red line). It can be seen that the calculated curves are almost identical in the central area of the graph, where all the rays starting within the CRL aperture converge, but vary widely outside this central region.

We can see from this graph that taking into account the CRL aperture severely limits CRL focusing properties when absorption is weak, compared with the analytical solution

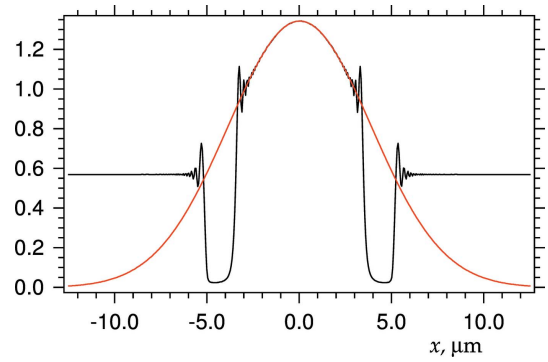

Figure 4
Curves of the relative X-ray intensity distribution at the third CRL example end, $E = 50$ keV and $L = L_o$. The black line is for the iterative calculation. The red line is for the continuous refraction approximation. The aperture $A = 10$ μm; the number of elements in the CRL $N_l = L/p = 301$.

because the real beam size at the end of the CRL is less than the effective aperture. If we neglect the aperture, we obtain an overestimation of the CRL focusing ability. In this case, under the discussed analytical approximation, the CRL virtualy focuses the beam outside the real beam size where it is not possible.

The iterative calculation requires a relatively large amount of computing time. However, within the central area, it leads to the same result as the analytical approach. On the other hand, the transverse beam profile at the end of the CRL can be easily found by calculating the trajectory corresponding to the aperture edge using formula (10) that takes into account the distance to the source.

Equation (10) reveals that in the limit of a very distant source ($\theta_0 = 0$) and for $L = L_o$ the transverse beam size A_0 at the CRL end due to refraction decreases to the value of $0.707A$. Thus, for $A = 10$ μm, we have $A_0 = 7.07$ μm – the same result as for the iterative calculation in Fig. 4. Therefore, to find an analytical solution which takes into account the CRL aperture, we need to consider the function (18) with $r_i = 0$, which we denote $G_0(x, x_o)$, and calculate the integral of type (21) but within finite limits calculated independently. As a result, we have a more accurate wavefunction described by the integral

$$G_1(x_i, x_o) = \int_{-A_0/2}^{A_0/2} \mathrm{d}x\; P(x_i - x, r_i)\, G_0(x, x_o). \tag{34}$$

The general analytic solution of (34) has no practical benefit due to its complexity. It is easier to calculate the integral numerically by applying the double Fourier transform using the fast Fourier transform algorithm. The following analytic expression is obtained under the linear in the γ approximation in the extreme case ($r_o \to \infty$) and only for the focus distance $r_i = r_f$, where $r_f = F_L C_L$.

Under these circumstances, integral (34) does not depend on x_o and can be written as

$$G_1(x) = \frac{P(x, r_i)}{C_L^{1/2}} \frac{A_0}{u_0} \int_0^{u_0} \mathrm{d}u \ \cos(u) \exp\left(-g u^2/u_0^2\right), \qquad (35)$$

where

$$u_0 = \frac{\pi A_0}{\lambda r_i} x, \quad g = \frac{\pi \gamma \alpha_L A_0^2}{4 \lambda r_i C_L}. \qquad (36)$$

The real-valued integral in (35) can be expressed in terms of the Fresnel integrals with complex arguments, but this is still inconvenient. Hence, let us consider limiting cases instead. When $g > 2$, the upper limit of the integral can be approximately substituted by infinity resulting in formula (26) for the relative intensity $I(x) = |G_1(x)|$. If $g < 2$, it is convenient to use the power series expansion of the exponent in terms of the parameter g. In this situation, all the integrals can be calculated, and the answer can be expressed as

$$G_1(x) = P(x, r_i) \frac{A_0}{C_L^{1/2}} \left[f_0(u_0) + \sum_{k=1}^{\infty} \frac{(-g)^k f_k(u_0)}{(2k+1)\, k!} \right], \qquad (37)$$

where $f_0(z) = \sin z/z$, and the other functions are calculated by means of the following recurrence relation,

$$f_k(z) = (2k+1) \left\{ f_0(z) - 2k \frac{\left[f_{k-1}(z) - \cos z \right]}{z^2} \right\}. \qquad (38)$$

The functions are defined in a way that $f_k(0) = 1$ for all the values of k.

It should be noted that equation (38) is inconvenient for the calculations since each new function is estimated with less accuracy. Therefore, completely inaccurate values may be obtained with its repetitive use.

At the same time, equation (38) allows us to obtain the power series for all functions $f_k(z)$ having now a relatively simple form,

$$f_k(z) = 1 + \sum_{n=1}^{\infty} \frac{(2k+1)(-z^2)^n}{(2k+2n+1)(2n)!}. \qquad (39)$$

The best numerical computation procedure is to choose the maximum value of the index k, for example m. Function $f_{\mathrm{m}}(z)$ is then obtained using power series (39), and the functions having $k < m$ can be calculated by the following recurrence relation,

$$f_{k-1}(z) = \cos(z) + \frac{z^2}{2k} \left[f_0(z) - \frac{f_k(z)}{2k+1} \right]. \qquad (40)$$

This formula provides accurate results for all the values of k, including $k = 0$, and it is usually enough to have $m = 10$ for all the values of the parameter g in formula (37).

Fig. 5 shows the intensity profile at the focus calculated for $E = 50$ keV by applying the method described in this section for the third CRL example having the number of elements $N_1 = 301$. The black curve corresponds to the real situation, when $g = 0.209$, and within the limits of the graph resolution matches the curve calculated under the iterative method based on formulas (32) and (33). The red curve is calculated for the case with no absorption when $g = 0$ and represents the analytic solution.

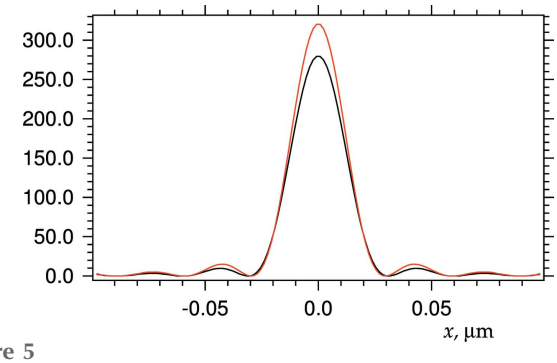

Figure 5
Curves of the X-ray radiation relative intensity distribution at the focal distance for the third CRL example, $E = 50$ keV and $L = L_o$. The black curve is for the case taking into account absorption; the red curve is for the case without absorption.

Comparing the curves, we can deduce that weak absorption slightly reduces the intensity but has almost no effect on the curve FWHM, which for zero absorption is determined as follows,

$$w_f = 0.886 \frac{\lambda r_f}{A_0}. \qquad (41)$$

This equation is valid for any photon energy E and is virtually the same as the one for the thin lens, except that for the long CRL the distance r_f is measured from its end and can be small. Another difference is that, instead of the aperture size, the transverse beam size A_0 at the end of the CRL is used, which is smaller than the aperture. Both parameters, r_f and A_0, are calculated analytically.

For the same CRL parameters as in Fig. 5 ($\lambda = 0.0248$ nm, $r_f = 0.845$ cm, $A_0 = 7.07$ μm) we have $w_f = 26$ nm obtained from equation (41). Curiously, the same result can be achieved by multiplying the beam size calculated without considering the aperture using formula (27) for the same wavelength by the factor $1.887 A_{\mathrm{e}}/A$. The latter can be easily verified if we substitute the value of A_{e} obtained from (25) and take into account that $F_L/A = r_f/A_0$.

Thus, the more accurate criterion for the situation in which the CRL aperture does not influence the result is $A_{\mathrm{e}} < 0.53A$. Hence, we cannot simultaneously decrease the absorption and the CRL aperture, as it is required by equation (31). The ratio $F_L/A = r_f/A_0$ allows us to rewrite equation (41) in a different form using the definitions of the parameters F_L and L_c, namely

$$w_f = \frac{0.886\, h}{S_L} w_c. \qquad (42)$$

Here, the parameters defined by equation (31) are used. If we define the CRL length for each photon energy E from the condition of the constant value of the parameter S_L, the beam size becomes weakly dependent on E.

Equation (42) shows that in the case of focusing at the CRL end when $L = 2L_o$ and $S_L = 1$, the beam size is slightly less than $w_c = 20$ nm. For the half of this length $L = L_o$, the beam size

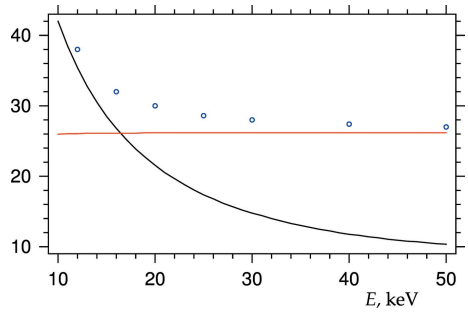

Figure 6
Dependence of the focused beam transverse size w_f (nm) from the photon energy for two approximations: taking into account absorption but without an aperture (black curve); and with aperture but without absorption (red curve) for the third CRL example and $L = L_o$. The blue markers show the accurate values according to equation (35).

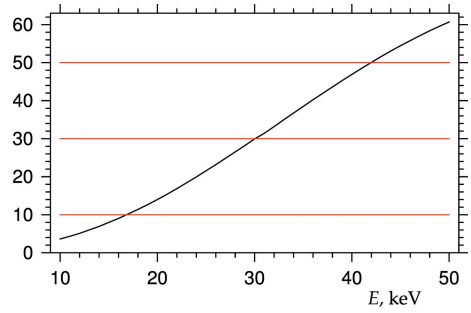

Figure 7
Dependence of the critical aperture A_1 (μm) from the photon energy E for $L = L_o$. See text for details.

is larger than w_c, namely 26 nm for $E = 50$ keV. In reality, absorption leads to further increasing the beam size, especially in the region where A_e is close to but less than $A/2$.

It is of interest to note that formula (42) under the outlined conditions is independent of the CRL aperture. Figure 6 presents the calculated transverse beam size at the focus, depending on photon energy E. The black curve was evaluated using formula (30), *i.e.* without taking into account the aperture but considering the absorption. The red curve was calculated for $L = L_o$ with the use of formula (42), *i.e.* taking into account the aperture but not taking into consideration the absorption. The blue markers show the accurate values according to equation (35). Note that for any energy the correct value is the greater one.

Figure 6 illustrates the following general conclusion. For any CRL aperture and small values of the photon energy E, approximation (27) without considering the aperture holds. As the energy E increases, photons absorption decreases, and the aperture starts to influence the result. Therefore, the calculations should be performed either under approximation (37) taking into consideration the aperture size or using more straightforward, though less accurate, equation (42) without taking into account the absorption.

We can determine the boundary between the two cases from the condition of the equality of equations (27) and (42). From analytical calculation we obtain that the CRL aperture affects the result when

$$A < A_1 = C_A \frac{h w_c}{\gamma}, \quad C_A = \frac{1.779}{S_L \alpha_L}, \tag{43}$$

and for the optimal situation ($L = L_o$) we have $C_A = 2.77$.

The parameter A_1 can be defined as the CRL critical aperture, meaning that an increase of the aperture above this value leads to the increased beam size at the focus. The value of A_1 increases with the increasing photon energy E. Figure 7 shows the dependence of the critical aperture A_1 on the photon energy E when $L = L_o$. From the graph, we can see that each of the described CRLs having aperture sizes of 10, 30 and 50 μm can focus X-rays down to 26 nm, but the lens with the smaller aperture does this in the broader energy range.

It is also interesting to consider the transverse beam size w_0 at the end of the CRL. If we ignore absorption but take into account the CRL aperture size, then we obtain $w_0 = A_0$, where $A_0 = AC_L$. In the opposite extreme case of hard absorption, we obtain $w_0 = w_a$, where w_a is the FWHM of the intensity Gaussian curve at the end of the lens according to the analytical theory,

$$w_a = 0.664 C_L \left(\frac{\lambda F_L}{\gamma \alpha_L}\right)^{1/2}. \tag{44}$$

It can be demonstrated that condition (43) is equivalent to the condition $A_0 < 2w_a$, where the coefficient 2 appears due to the FWHM difference of the Gaussian function and its square.

5. Conclusion

The main findings to be drawn from the presented analysis are as follows.

X-ray compound refractive lenses (CRLs) having large aperture size and optimal length L, approximately equal to $L_o = 0.28A/\delta^{1/2}$, strongly absorb the radiation for the low photon energies E (less than 20 keV), which leads to the decreasing effective aperture for a relatively high focal length. Consequently, the transverse beam size at the focus has a relatively high value, while the CRL aperture does not influence the result and merely increases the optimal length and the focal length of the lens.

It is necessary to switch to the CRLs with the smaller aperture and use harder radiation ($E > 20$ keV) in order to reduce the beam size at the focus. In this instance, the absorption impact on the focusing process decreases, and the beam size inside the CRL is restricted by the CRL aperture. For the CRL length $L = L_o$, the focused beam size no longer depends on both the aperture and the energy. It is approximately equal to the critical size $w_c = \lambda/(8\delta)^{1/2}$ obtained for the first time by Bergemann *et al.* (2003) as the smallest achievable beam size for any focusing method.

The previous conclusion is contrary to the widespread view that materials consisting of light atoms (*e.g.* beryllium, diamond, aluminium, silicon) have an advantage for the production of CRLs. In fact, such materials are only effective

for soft energies. In contrast, for hard X-rays, heavy-atom materials are promising, *e.g.* nickel.

Funding information

This work was supported by the Russian Foundation for Basic Research, project 19-29-12043 mk.

References

Argunova, T. S. & Kohn, V. G. (2019). *Phys. Usp.* **62**, 602–616.
Bergemann, C., Keymeulen, H. & van der Veen, J. F. (2003). *Phys. Rev. Lett.* **91**, 204801.
Cooley, J. W. & Tukey, J. W. (1965). *Math. C*, **19**, 297–301.
Grigoriev, M., Shabelnikov, L., Yunkin, V., Snigirev, A., Snigireva, I., Di Michiel, M., Kuznetsov, S., Hoffmann, M. & Voges, E. (2001). *Proc. SPIE*, **4501**, 185–192.
Kohn, V. G. (2002). *JETP Lett.* **76**, 600–603.
Kohn, V. G. (2003). *J. Exp. Theor. Phys.* **97**, 204–215.
Kohn, V. G. (2009). *J. Surface Investig.* **3**, 358–364.
Kohn, V. G. (2012). *J. Synchrotron Rad.* **19**, 84–92.
Kohn, V. G. (2015). *X-ray Refraction Parameters*, http://kohnvict.ucoz.ru/jsp/2-irpar.htm.
Kohn, V. G. (2017). *J. Synchrotron Rad.* **24**, 609–614.
Kohn, V. G. (2018). *J. Synchrotron Rad.* **25**, 425–431.
Kohn, V. G., Snigireva, I. & Snigirev, A. (2014). *J. Synchrotron Rad.* **21**, 729–735.
Lengeler, B., Schroer, C., Tümmler, J., Benner, B., Richwin, M., Snigirev, A., Snigireva, I. & Drakopoulos, M. (1999). *J. Synchrotron Rad.* **6**, 1153–1167.
Lyubomirskiy, M., Snigireva, I., Kohn, V., Kuznetsov, S., Yunkin, V., Vaughan, G. & Snigirev, A. (2016). *J. Synchrotron Rad.* **23**, 1104–1109.
Protopopov, V. V. & Valiev, K. A. (1998). *Opt. Commun.* **151**, 297–312.
Sanchez del Rio, M., Canestrari, N., Jiang, F. & Cerrina, F. (2011). *J. Synchrotron Rad.* **18**, 708–716.
Schroer, C. G., Kuhlmann, M., Hunger, U. T., Günzler, T. F., Kurapova, O., Feste, S., Frehse, F., Lengeler, B., Drakopoulos, M., Somogyi, A., Simionovici, A. S., Snigirev, A., Snigireva, I., Schug, C. & Schröder, W. H. (2003). *Appl. Phys. Lett.* **82**, 1485–1487.
Schroer, C. G. & Lengeler, B. (2005). *Phys. Rev. Lett.* **94**, 054802.
Snigirev, A., Kohn, V., Snigireva, I. & Lengeler, B. (1996). *Nature*, **384**, 49–51.
Snigirev, A., Snigireva, I., Kohn, V., Kuznetsov, S. & Schelokov, I. (1995). *Rev. Sci. Instrum.* **66**, 5486–5492.
Snigirev, A., Snigireva, I., Kohn, V., Yunkin, V., Kuznetsov, S., Grigoriev, M. B., Roth, T., Vaughan, G. & Detlefs, C. (2009). *Phys. Rev. Lett.* **103**, 064801.
Snigirev, A., Snigireva, I., Lyubomirskiy, M., Kohn, V., Yunkin, V. & Kuznetsov, S. (2014). *Opt. Express*, **22**, 25842–25852.